ECOGRAPHY

Research Article

Satellite hindcasts of foliar traits reveal a subtle but consistent relaxation of conservativeness in a biodiverse mountain grassland over the last four decades

Renata Maia[1,2], **Milton Barbosa**[1,2], **Daniel Negreiros**[1], **Geraldo Wilson Fernandes**[1,3],
Yadvinder Malhi[4,5] **and Jesus Aguirre-Gutiérrez**✉[2,5]

[1]Department of Genetic, Ecology & Evolution, Federal University of Minas Gerais, Belo Horizonte, Brazil
[2]Biodiversity and Earth Observation, Environmental Change Institute, School of Geography and the Environment, University of Oxford, Oxford, UK
[3]Knowledge Center for Biodiversity, Belo Horizonte, Brazil
[4]Environmental Change Institute, School of Geography and the Environment, University of Oxford, Oxford, UK
[5]Leverhulme Centre for Nature Recovery, University of Oxford, Oxford, UK

Correspondence: Jesus Aguirre-Gutiérrez (jesus.aguirregutierrez@ouce.ox.ac.uk)

Ecography
2026: e07634
doi: 10.1002/ecog.07634
Subject Editor: Vigdis Vandvik
Editor-in-Chief:
Dominique Gravel
Accepted 27 February 2026

Projected warming and drying raise concerns about the resilience of stress-adapted ecosystems, including the Brazilian Campo Rupestre, an exceptionally biodiverse mountaintop grassland mosaic on ancient, nutrient-poor substrates. Here, we combine field-based trait data and long-term remote sensing to assess the functional structure and temporal dynamics of these communities. Using foliar trait measurements from 247 vegetation plots across five contrasting habitats, we 1) quantify contemporary community-level functional structure, 2) evaluate how edaphic and climatic filters shape spatial variation in community-weighted foliar traits, and 3) reconstruct multi-decadal trait trajectories by hindcasting from long-term Landsat reflectance (1984–2022). Contemporary communities occupy a narrow and predominantly conservative region of the leaf-economic trait spectrum, yet habitats differ in their functional positions within CSR strategy space, indicating non-uniform trait coordination despite overall conservatism. Soil texture and acidity define the primary conservative–acquisitive axis of trait variation, while climatic water balance acts as a secondary modulator; together, these predictors explain 39% of the spatial variation in community-weighted traits. Contrary to expectations of increasing conservatism under progressive climatic stress, Landsat-based hindcasts reveal only modest temporal reorganisation. Specific leaf area and leaf area increase across habitats, while leaf dry matter content declines slightly, indicating a subtle relaxation of conservative trait expression. Temporal changes are small relative to the pronounced spatial differentiation, suggesting strong functional inertia in this OCBIL system. Overall, Campo Rupestre communities persist within a

NORDIC SOCIETY OIKOS
www.ecography.org

---

conservative functional domain while exhibiting fine-scale, habitat-dependent differentiation structured by enduring soil and water-balance gradients.

Keywords: functional traits, leaf economics spectrum, OCBILs, rupestrian grasslands, satellite-based reconstructions, spectral reflectance

Introduction

Climate change is reshaping ecosystems worldwide by altering water balance, thermal regimes and the conditions under which plant communities persist (Rummukainen 2012, Trenberth et al. 2014, Povak and Manley 2024). Because plants respond to these pressures through coordinated physiological and morphological adjustments, functional traits play a central role in determining resource use, stress tolerance and competitive performance (Querejeta et al. 2021). The capacity of plant communities to withstand increasing environmental stress therefore depends on their functional composition and on the extent to which species can adjust their traits through phenotypic plasticity. When plasticity is insufficient, environmental filtering may favour species with alternative trait combinations, reorganising community structure (Ma et al. 2017). Evidence from tropical ecosystems indicates that functional adjustment may be slower than the pace of climate change, raising concerns about adaptive lags and reduced ecological resilience (Aguirre-Gutiérrez et al. 2025). These risks are particularly relevant in naturally stressful ecosystems, where species are well adapted to harsh conditions but often operate with narrow physiological safety margins (Lambers et al. 2008). Understanding how traits vary and reorganise across environmental gradients is therefore essential for anticipating future biodiversity trajectories under ongoing climatic intensification. Recent advances in remote sensing now allow these functional traits to be estimated and tracked over time, providing new opportunities to assess not only spatial patterns but also long-term trajectories of community functional composition (Kattenborn et al. 2017, Wang et al. 2020, Aguirre-Gutiérrez et al. 2021).

Three key foliar traits – specific leaf area (SLA), leaf dry matter content (LDMC) and leaf area (LA) – form the core axis of the leaf economics spectrum (LES), a robust trait-based framework supported by consistent patterns of covariation observed across species, biomes, and environmental gradients, reflecting fundamental tradeoffs in resource acquisition and conservation (Wright et al. 2004, Díaz et al. 2016). These same traits also underpin ecological strategies in Grime's CSR framework, which complements the LES by linking functional traits to whole-plant responses to competition, stress and disturbance (Grime 1977, Pierce et al. 2017). Because SLA, LDMC and LA respond predictably to gradients in soil texture, nutrient availability and water balance, they provide a strong basis for assessing how fine-scale environmental filters shape community composition. Understanding their spectral behaviour also allows for estimation from satellite-based multiband reflectance, expanding their applicability across spatial and temporal scales previously inaccessible to trait-based ecological inference (Kattenborn et al. 2017, Wang et al. 2020, Aguirre-Gutiérrez et al. 2021).

Current approaches to anticipate plant responses to climate change often assume that species will shift their distributions to track suitable climate (Huntley et al. 2010, Corlett and Tomlinson 2020). However, in landscapes shaped by pronounced edaphic controls, the capacity of species to track shifting climates through migration may be severely constrained. For edaphically specialized plants, substrate limitations restrict dispersal and reduce the availability of suitable habitat (Barbosa et al. 2015), a pattern characteristic of 'old, climatically buffered, infertile landscapes' (OCBILs), which have historically acted as refugia during climatic oscillations (Hopper 2009, 2021, Rapini et al. 2021). The Brazilian Campo Rupestre is a prominent example of an OCBIL system, occurring on ancient mountaintops and comprising a fine-scale mosaic of substrates ranging from quartzitic to ferruginous, which generate sharp contrasts in nutrient availability and water-holding capacity (Fernandes 2016, Silveira et al. 2020). This fine-scale edaphic heterogeneity imposes environmental filtering, favouring predominantly stress-tolerant species with conservative leaf-trait profiles (Negreiros et al. 2014, Silveira et al. 2016, Caminha-Paiva et al. 2021, Tameirão et al. 2021, Rios et al. 2022).

Despite the dominance of conservative strategies, substantial functional variation persists within the Campo Rupestre (Negreiros et al. 2014, Caminha-Paiva et al. 2021, Paiva et al. 2025) because the sharp edaphic contrasts that characterise the system, combined with fine-scale microclimatic differences related to exposure – such as variation in drainage and sun exposure – generate strong local environmental filters (Fernandes 2016, Silveira et al. 2016). Together, these gradients have the potential to structure community-level foliar traits along the conservative–acquisitive axis, producing spatially organised variation even within a predominantly conservative system. In addition, although these species are well adapted to these substrates, the Campo Rupestre is increasingly exposed to pressures from climate change and human disturbance, raising concerns about long-term functional resilience (Jacobi et al. 2007, Fernandes et al. 2020, Moura et al. 2023). Understanding the extent and drivers of this variation is essential for evaluating the sensitivity and resilience of Campo Rupestre communities under ongoing environmental change. Yet, it remains unclear how foliar traits vary across contrasting substrates of the Campo Rupestre, and whether community-level trait composition has shifted over recent decades – knowledge gaps that persist largely because long-term trait datasets are rare.

Spectral remote sensing has increasingly enabled the estimation of these traits from multispectral reflectance, offering a scalable approach to map functional strategies across landscapes and to reconstruct potential temporal shifts in community-level traits (Kattenborn et al. 2019, Aguirre-Gutiérrez et al. 2021, Ordway et al. 2022). Here, we integrate a large field-collected dataset from 247 plots with long-term satellite reflectance data to investigate spatial and temporal patterns of foliar functional traits (SLA, LDMC and leaf area) in the Campo Rupestre. We test the following hypotheses: H1: conservative foliar trait profiles (low SLA, high LDMC, small LA) currently predominate across the Campo Rupestre, reflecting the typical constraints of OCBIL systems. However, we expect detectable variation along the conservative–acquisitive axis driven by fine-scale environmental heterogeneity within the landscape. We evaluate this hypothesis by quantifying variation in community-weighted mean (CWM) trait values and by mapping their functional positions within CSR strategy space. H2: spatial variation in foliar traits (SLA, LDMC and LA) arise from underlying environmental gradients. We expect soil properties to be the primary drivers of conservative–acquisitive shifts, with fine-scale climatic variability further modulating trait expression. We test this hypothesis by relating CWM traits to combined edaphic and climatic predictors and by evaluating joint trait–environment structure in multivariate space. H3: present-day communities exhibit more conservative trait profiles than in the past, consistent with increasing warming and drought stress over recent decades. We evaluated this hypothesis by reconstructing temporal trajectories of CWM foliar traits through hindcasting from satellite reflectance. Models trained on present-day SLA, LDMC and LA were applied to four decades of spectral data, allowing the quantification of directional temporal trends in community-level trait composition and the assessment of long-term shifts towards more conservative trait profiles. Together, these hypotheses aim to disentangle how environmental filtering and recent environmental pressures shape both spatial and temporal patterns of foliar traits in this stress-adapted OCBIL ecosystem.

Material and methods

Dataset description and study area

Plant functional traits and soil data analysed in this study were compiled from multiple previously published and ongoing studies (Negreiros et al. 2014, Caminha-Paiva et al. 2021, Tameirão et al. 2021, Paiva et al. 2025, Negreiros et al. unpubl., Paiva et al. unpubl.). These datasets were integrated into a single database and reanalysed to investigate patterns of foliar trait variation across environmental gradients, with a focus on community-level functional responses.

The study encompasses Campo Rupestre vegetation from the southern portion of the Espinhaço Mountain Range, Minas Gerais, Brazil (Supporting information). The database includes records from Vellozia Natural Reserve, Serra do Cipó, in the municipality of Santana do Riacho (19°17′08.5″S, 43°35′44.2″W; Negreiros et al. unpubl., Paiva et al. unpubl.); from Serra do Intendente State Park and outside, in the municipality of Conceição do Mato Dentro (19°06′08.5″S, 43°37′13.4″W; Paiva et al. 2025, Paiva et al. unpubl.). In addition, the dataset includes sites from the Quadrilátero Ferrífero, namely from Serra do Rola-Moça State Park (20°03′07″S, 44°00′06″W; Tameirão et al. 2021); Morro do Pilar municipality (19°13′09.5″S, 43°23′20.9″W; Paiva et al. 2025); Serra da Calçada State Park (20°08′11.9″S, 43°24′23.9″W; Caminha-Paiva et al. 2021); and Catas Altas municipality (20°07′05.2″S, 43°59′42.0″W; Paiva et al. 2025).

The Campo Rupestre is an ancient ecosystem typically occurring at elevations above 900 m a.s.l. It is characterised by a heterogeneous mosaic of herbaceous and shrub-dominated vegetation adapted to shallow, acidic, and nutrient-poor soils (Fernandes 2016). The regional climate across these mountaintop environments is mesothermal with dry winters and hot to temperate summers. According to the Köppen climate classification, sites located in Serra do Cipó, Serra do Intendente, Serra do Rola-Moça, Serra da Calçada State Parks and Catas Altas fall within the CWb subtype, whereas Morro do Pilar and Conceição do Mato Dentro correspond to CWa (Alvares et al. 2013). Climate seasonality is pronounced, with most precipitation occurring between November and April and a marked dry season extending from May to October (Madeira and Fernandes 1999). Our analysis of long-term climate datasets (TerraClimate, 1984–2022; Abatzoglou et al. 2018) indicates a consistent shift toward warmer and drier conditions across the region. Maximum temperatures increased by approximately 1.1–1.2°C in the dry season and ~ 0.8°C in the wet season. Water-balance indicators also shifted toward drier conditions, with a steady rise in the climatic water deficit (CWD) and progressively more negative Palmer drought severity index (PDSI) values, particularly after the early 2000s. Details on TerraClimate data extraction, spatial resolution and temporal aggregation are provided in the Supporting information. Together, these trends describe a long-term warming and drying trajectory for the Campo Rupestre (Supporting information).

The Campo Rupestre landscape is characterised by a fine-scale mosaic of habitats shaped by strong variation in substrate and edaphic conditions (Fernandes 2016). The dataset analysed here includes plots distributed across five distinct habitat types commonly recognized in this system, which differ in substrate, topographic setting, and visually apparent soil texture: 1) Quartzitic Grassland (including both stony and sandy grasslands); 2) Rock Outcrop; 3) Candeal (dominated by the *Eremanthus* spp.); 4) Ironstone Grassland (including both Canga couraçada and Canga nodular), and 5) Peat bog (Supporting information). Across these habitats, the compiled dataset comprises multiple sampling sites distributed throughout the study regions, with sampling effort varying according to habitat availability (two to seven sites per habitat; Supporting information). At each site, vegetation and soil information was recorded in approximately ten 100 m^2 plots (10 × 10 m) per site, spaced at least 10 m apart to reduce fine-scale spatial autocorrelation. Plots were originally established within habitat patches and constrained to areas representative of each habitat's physiognomy and substrate conditions. In total, the dataset includes 247 plots spanning all habitats and study regions.

Vegetation traits

Vegetation sampling across the study sites followed standardized protocols as described in the original studies from which the data were compiled and was conducted at the plot level (100 m^2 plot), recording all vascular plant species occurring within each plot, including both herbaceous and shrub components. In most surveys, vegetation was sampled as a single, unified community, without prior separation between growth forms. In cases where herbaceous taxa contributed negligibly to community-level dominance and therefore had minimal influence on CWM trait values, only the woody component was retained for the present analyses. Taxonomic identification was supported by voucher specimens and validated by specialist taxonomists, and vouchers were deposited in the BHCB Herbarium (Federal University of Minas Gerais) and the BHZB Herbarium (Belo Horizonte Botanical Garden), following standard herbarium procedures.

To define the subset of taxa included in functional trait analyses, species were ranked by their importance value index (IVI), calculated from relative density, relative frequency for all species, with relative dominance (basal area) included only for woody and subshrub species. Within each site, species contributing cumulatively to ≥ 80% of total IVI were selected for trait measurements, resulting in 321 species included in the functional trait analyses and ensuring that the most structurally important species were represented.

Functional trait measurements followed standardized protocols (Pérez-Harguindeguy et al. 2013). Trait sampling was conducted at the site level, with each site representing a spatial replicate of a given habitat and comprising multiple plots. For each species, branches from 5–6 healthy, sun-exposed individuals were collected during the wet season between 07:00 and 10:00 h to minimize diurnal variation. In the field, branches were sprayed with water to prevent dehydration, placed in sealed plastic bags, and transported to the laboratory (Caminha-Paiva et al. 2021). In the laboratory, a ~ 5 cm segment was removed from the terminal portion of each branch under water, after which branches were placed in water containers and kept in the dark for at least 2 h to allow leaf rehydration. Following rehydration, two to three fully expanded, undamaged leaves per branch were selected and blotted dry to measure turgid fresh mass using an analytical balance (precision of 0.1 mg). Leaves were then scanned in a fully hydrated state, and leaf area (LA, mm^2) was quantified from scanned images using ImageJ software. Leaves were oven-dried at 70°C for a minimum of 72 h to determine leaf dry mass (LDM). Specific leaf area (SLA, $mm^2\ mg^{-1}$) was calculated as the ratio of LA to LDM. Leaf dry matter content (LDMC, %) was calculated as (dry mass/fresh mass) × 100. When the same species occurred in more than one site, functional traits were measured separately for each site.

Community-level functional composition was quantified using CWM calculated at the plot level for each functional trait (LA, SLA, LDMC). CWM values were weighted by species relative dominance, quantified as relative cover within each plot and rescaled to sum to 100%. This weighting approach was applied consistently to both herbaceous and shrub species and was used to represent plot-level functional composition.

Edaphic variables

Soil physical and chemical properties were analysed following standardized protocols applied in the original studies. At each plot, we collected five bulk soil subsamples (~ 300–500 g each) at 0–20 cm depth (four corners and the plot centre), which were homogenized into a single composite sample (~ 1.5–2.5 kg). All analyses followed standard protocols established by the Brazilian Agricultural Research Corporation – EMBRAPA (Silva et al. 1999, Donagemma et al. 2017). Soil texture was determined using the pipette method for the silt and clay fractions (%), and the sieving method for coarse and fine sand fractions (%). Soil pH was measured in water using a 1:2.5 (w/v) soil-to-water ratio. Exchangeable Al^{3+}, Ca^{2+} and Mg^{2+} were extracted using 1 M KCl following standard protocols, and concentrations were expressed in $cmol_c\ dm^{-3}$. For phosphorus (P, $mg\ dm^{-3}$) and potassium (K, $mg\ dm^{-3}$), the Mehlich-1 extractor method was applied. Additionally, we assessed potential acidity (H+Al) using a 0.5 $mol\ l^{-1}$ calcium acetate solution at a pH of 7.0, evaluated cation exchange capacity (CEC), and quantified organic matter (OM) as organic carbon multiplied by a factor of 1.724 (Walkley and Black 1934).

Climate and hydrological variables from TerraClimate and ECOSTRESS

We used TerraClimate, a gridded climate dataset (Abatzoglou et al. 2018), to obtain monthly maximum temperature (MaxT) and climatic water deficit (CWD) for each sampling plot over the period 2019–2022. TerraClimate provides global land surface data at ~ 4 km spatial resolution, combining high-resolution climatological interpolation from WorldClim with time-varying data from CRU Ts4.0 and the Japanese 55-year Reanalysis (JRA-55). We accessed these datasets via the Google Earth Engine (GEE) JavaScript API catalogue. At present, no long-term climate datasets are available for this region at a spatial resolution comparable to the scale of our vegetation plots.

In addition, we incorporated plant-water interaction metrics derived from the ECOSTRESS mission (Ecosystem Spaceborne Thermal Radiometer Experiment on Space Station). ECOSTRESS provides thermal infrared observations at ~ 70 m spatial resolution every 1 to 5 days (Fisher et al. 2020), enabling the detection of short-term and hydrological responses. We extracted three key variables: the Evaporative Stress Index (ESI), Water Use Efficiency (WUE), and Evapotranspiration (ET), derived from Level 4 products processed using the DisALEXI energy balance model (Anderson et al. 2011). ECOSTRESS data obtained via

NASA's AppEEARS platform and covered the period from January 2019 to December 2022, overlapping with the collection of functional trait and soil data. Additional details on data derivation and processing are provided in the Supporting information.

Spectral data for trait modelling and temporal back-projection

Harmonized Landsat 8 and Sentinel-2 (HLS) – Spectral predictors and model training

We used surface reflectance data from Harmonized Landsat 8 and Sentinel-2 (HLS) to train predictive models of community-level functional traits. For each plot, spectral reflectance values and vegetation indices were extracted for the period 2019–2022, using a 15 m buffer around plot coordinates. A 15 m buffer was used to reduce geolocation uncertainty and mixed-pixel effects while remaining consistent with the spatial resolution of HLS and Landsat surface reflectance products. Data were accessed via the GEE and filtered for high-quality pixels (cloud probability < 5%) (Crawford et al. 2023). Relevant spectral bands and vegetation indices were used to train Random Forest regression models predicting the CWM of functional traits. Model performance was evaluated using independent test data and standard accuracy metrics (R^2, RMSE, MAE). Model performance indicated sufficient predictive accuracy to support the intended temporal analyses of community-level functional traits (see the Supporting information for the full list of bands and indices).

Landsat 5, 7 and 8 – Historical trait projection

To reconstruct temporal changes in vegetation properties, we analysed a 39-year time series of Landsat 5, 7 and 8 surface reflectance (1984–2022), using the Tier 1 Level-2 product. For each plot, reflectance values were extracted within a 15 m buffer using the *reduceRegions()* function in GEE, applying strict cloud masking (cloud probability < 5%). The spectral time series were used to hindcast community-level trait values using Random forest models trained with HLS data. This hindcasting approach assumes that the relationships between spectral predictors and community-level trait expression remain stable through time. Additional details on preprocessing are provided in the Supporting information.

Statistical analysis

All analyses and figures were produced in R ver. 4.3.0 (www.r-project.org), with colours selected from the ColorBrewer 'Set1' qualitative palette (https://colorbrewer2.org) to ensure visual accessibility. Model assumptions were checked through diagnostic plots of residuals, including homoscedasticity, normality, and autocorrelation. All continuous predictors were standardised (mean = 0, SD = 1) prior to model fitting to improve coefficient interpretability and model convergence (Schielzeth 2010). The data used in this study are publicly available on Zenodo (Maia et al. 2026).

To test H1, we assessed whether community-level foliar traits across the Campo Rupestre are consistent with conservative functional profiles expected for OCBIL systems and whether these traits vary among habitats. We fitted generalised least squares (GLS) models for each trait (SLA, LA and LDMC), with habitat type included as a fixed effect. SLA and LA were $\log_{10}$-transformed to improve residual normality and homoscedasticity. To account for spatial autocorrelation among plots, we tested alternative correlation structures based on geographic coordinates using the *gls()* function from the 'nlme' package. Model selection was guided by AIC and BIC, with the exponential spatial correlation structure (corExp) consistently providing the best fit. Estimated marginal means were obtained using the *emmeans()* function from the emmeans 'package' (Lenth 2025), applying Tukey's adjustment for multiple comparisons and using the residual degrees of freedom for inference.

To aid interpretation, we additionally visualised plots in a trivariate trait space (CWM of SLA, LDMC and LA) and mapped their functional positions within CSR strategy space. CSR scores were assigned using the StrateFy tool (Pierce et al. 2017), which transforms and scales species-level of SLA, LDMC and LA values based on a globally calibrated trait database. These transformed values are projected into a CSR triangle using a principal component analysis (PCA) derived from global trait distributions, generating continuous proportional scores for C, S and R that sum to 100% for each species. We then calculated CWMs of these CSR scores for each plot, integrating species strategies with their relative abundances using the 'FD' package (Laliberté et al. 2014).

To test H2, that spatial variation in foliar traits is structured by environmental gradients, we first used redundancy analysis (RDA) using the *rda()* function from the 'vegan' package, to evaluate the joint multivariate structure of trait–environment relationships. Scaled CWM traits (Log_SLA, Log_LA and LDMC) were used as response variables and constrained by the full set of edaphic and climatic predictors. Multicollinearity among predictors was assessed prior to analysis (Supporting information), retaining soil-texture variables (CS, clay, FS), fertility and acidity metrics (CEC, AlSat, H + Al, pH, P, K), and hydric and thermal stress variables (CWD, MaxT, WUE, ESI). For the RDA analyses, the significance of the global model, constrained axes, and individual predictors was assessed using permutation tests (999 permutations).

Following the multivariate analysis, we evaluated trait-specific responses by fitting GLS using *gls()* function from the 'nlme' package (Pinheiro et al. 2025) for Log_SLA, Log_LA and LDMC. Each model included the same set of screened edaphic and climatic predictors, with habitat (five habitat types) included as a fixed effect, and incorporated an exponential spatial correlation structure (corExp) to account for spatial autocorrelation. Fixed-effect coefficients and their 95% confidence intervals were obtained using confint(), and post hoc comparisons among habitat types were conducted using Tukey-adjusted contrasts implemented in the 'emmeans' package (Lenth 2025).

To test H3, which posits that present-day communities exhibit more conservative trait profiles than in the past, we trained Random forest regression models (Liaw and Wiener 2002) to predict CWMs of SLA, LA and LDMC using reflectance-based environmental predictors from 2019-2022 period. Trait values were measured once per plot; given the conservative nature of this vegetation (slow growth, long leaf lifespan, low trait plasticity), we assumed temporal stability in trait–environment and used the trained models to hindcast trait values based on reflectance data from 1984 to 2022. This assumption is consistent with evidence in trait–environment relationships in OCBIL vegetation are primarily shaped by long-term evolutionary filtering rather than short-term plastic responses. Predictors included surface reflectance (blue, green, red, NIR, Swir1, Swir2), vegetation indices (NDVI, MSAVI, GLI, NDMI), and altitude. Spectral data were derived from harmonised Landsat and Sentinel-2 imagery. All predictors corresponded to the 2019–2022 period aligning with trait sampling.

Data were stratified by season and habitat and split into training (80%) and testing (20%) sets using stratified sampling *createDataPartition()*, using 'caret' package (Kuhn 2008). A Mahalanobis distance filter was applied to remove atypical environmental combinations based on the 99.9th percentile of the chi-square distribution. Random forests were fitted for each trait using 500 trees (ntree = 500), using 'randomForest' package, and model performance was evaluated via R^2, root mean square error (RMSE), and mean absolute error (MAE). Variable importance was assessed using %IncMSE and IncNodePurity (Supporting information). Validated models were then applied to historical environmental data (1984–2022), using harmonised Landsat sensors (Landsat 5, 7 and 8), to hindcast monthly CWMs of SLA, LA, and LDMC for each plot over four decades.

To reconstruct temporal trajectories of CWM traits and to test for directional temporal trends consistent with increasing functional conservatism, we fitted linear mixed-effects models using 'nlme' package, with year, habitat, and their interaction as fixed effects, polygon identity as a random intercept, and an exponential spatial correlation structure (corExp) based on geographic coordinates. For these mixed-effects models, we report marginal (R^2m) and conditional (R^2c) coefficients of determination following (Nakagawa and Schielzeth 2013), which quantify the variance explained by fixed effects alone and by the full model (fixed and random effects combined), respectively. Predicted trait values were extracted for each habitat in 1984 and 2022 to summarise the magnitude and direction of long-term changes in SLA, LA and LDMC, providing a direct comparison between historical and present-day community trait profiles. Although reflectance-based predictors were used, trait trajectories reflect shifts in community-level functional composition inferred from models trained on independent field-measured traits and constrained to observed environmental space, rather than direct temporal trends in spectral indices.

Results

Contemporary variation in foliar traits and CSR strategies across Campo Rupestre habitats

Leaf traits varied among vegetation types in the Campo Rupestre. SLA was lowest in Rock Outcrop and Ironstone Grassland, where values were 37% and 34% lower than in Candeal ($F_{4,242} = 2.841$, $p = 0.02$, Fig. 1a). Quartzitic Grassland and Peat bog showed intermediate SLA, with no significant contrasts relative to other habitats. LA also differed among vegetation types ($F_{4,242} = 12.715$, $p < 0.001$, Fig. 1b). Ironstone Grassland and Peat bog showed smallest leaves, with LA 79% and 75% lower than in Candeal. Rock Outcrop exhibited the largest LA, exceeding Ironstone Grassland, Peat bog, and Quartzitic Grassland, while Quartzitic Grassland occupied an intermediate position, differing only Ironstone Grassland. LDMC likewise displayed habitat differentiation ($F_{4,242} = 7.249$, $p < 0.001$, Fig. 1c). LDMC was highest in Quartzitic Grassland, with values approximately 20%, 14%, and 10% higher than in Candeal, Peat bog, and Ironstone Grassland, respectively. Rock Outcrop showed intermediate LDMC, overlapping with both Quartzitic Grassland and the lower-LDMC habitats.

CSR strategy space showed broadly similar functional profiles across four habitat types – Rock Outcrop, Ironstone Grassland, Quartzitic Grassland and Candeal – with plots forming narrow clusters near the stress (S) vertex and negligible contributions from the competitive (C) dimension (Fig. 1d, e, g, h). In contrast, Peat bog exhibited a much wider spread along the stress–ruderal (S–R) axis, including plots with elevated R scores and moderate C contributions, indicating markedly greater within-habitat functional variability (Fig. 1f).

Edaphic and climatic filters structure foliar trait variation across the Campo Rupestre

Environmental predictors accounted for 39% of the variation in community-level foliar traits (Fig. 2a, Supporting information). Two dominant RDA axes structured this constrained variation. The first axis (52%) reflected an edaphic gradient from clay-rich, acidic soils to sandier substrates. SLA, and to a lesser extent LA, increased toward clay-rich and highly acidic sites characterised by high AlSat, H+Al and CEC, whereas LDMC was associated with the sandier end of this gradient. The second axis (38%) captured a gradient of water and thermal stress. Higher CWD, ESI, MaxT and WUE loaded positively on this axis, indicating that warmer and drier conditions were associated with more conservative leaf trait combinations, characterised by higher LDMC and lower SLA.

Habitat types occupied distinct regions of this constrained trait-environment space. Ironstone Grassland were concentrated towards the sandier and more water-limited portion of the ordination, whereas Peat bog was associated with wetter, clay-rich conditions. Rock Outcrop and Quartzitic Grassland exhibited intermediate distributions, while Candeal plots formed a cohesive group within the sandy, moderately water-stressed region of the ordination (Fig. 2a).

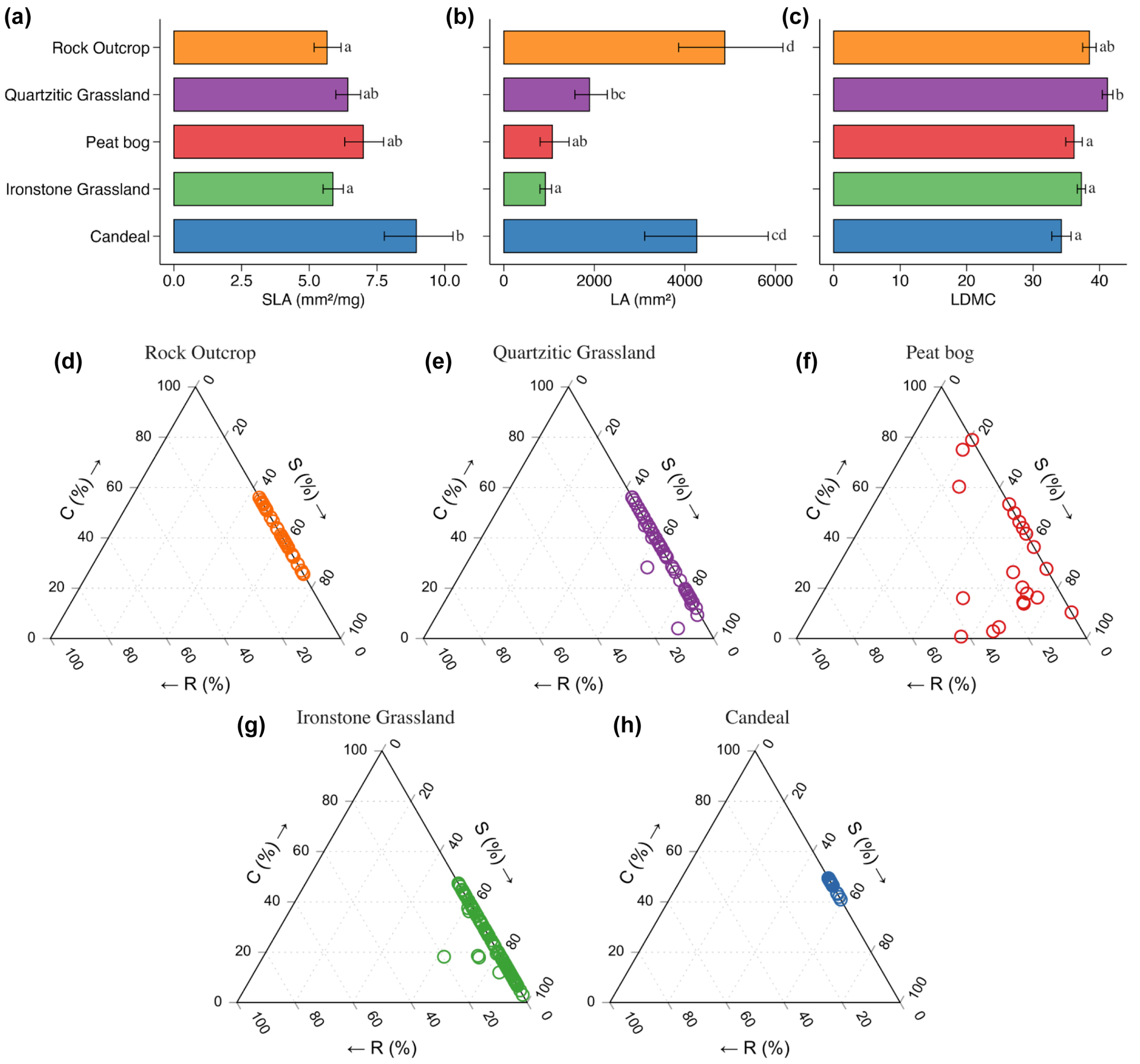

Figure 1. Variation in leaf traits and CSR functional strategy composition across habitats in the Campo Rupestre, an OCBIL (Old, Climatically buffered, Infertile landscapes) system. (a– c) Model-predicted means (± 95% CI) of specific leaf area (SLA), leaf area (LA), and leaf dry matter content (LDMC), estimated using spatial GLS models for each habitat type. Letters indicate Tukey post hoc differences. (d–h) Relative proportions (%) of competitive (C), stress-tolerant (S), and ruderal (R) strategies derived from CWM of leaf traits using the CSR ordination framework. Each point represents a vegetation plot.

Spatial variation in foliar traits across the Campo Rupestre was structured by gradients in soil properties and climatic water balance (Fig. 2b–d). SLA showed a positive association with soil pH ($F_{1,233}=15.45$, $p < 0.001$, $\beta=0.074$) and a negative association with ESI ($F_{1,233}=11.86$, $p < 0.001$, $\beta=-0.137$). LA was negatively associated with H_Al ($F_{1,233}=1.38$, $p=0.004$, $\beta=-0.432$) and ESI ($F_{1,233}=18.92$, $p < 0.001$, $\beta=-0.383$). In contrast, LA increased with AlSat ($F_{1,233}=35.54$, $p < 0.001$; $\beta=0.185$) and WUE ($F_{1,233}=6.30$, $p=0.050$, $\beta=0.242$). LDMC had positive associations with AlSat ($F_{1,233}=18.49$, $p=0.001$, $\beta=1.254$) and MaxT ($F_{1,233}=3.29$, $p=0.016$, $\beta=1.408$), but negative associations with H_Al ($F_{1,233}=23.75$, $p < 0.001$, $\beta=-1.512$) and FS ($F_{1,233}=0.21$, $p=0.012$, $\beta=-1.95$).

Retrospective trait projections reveal increasing SLA and declining LDMC in Campo Rupestre vegetation

Predicted SLA values, derived from spectral reflectance and retrospectively projected from 1984 to 2022, showed habitat-dependent positive temporal trajectories ($\chi^2=294.7$, p

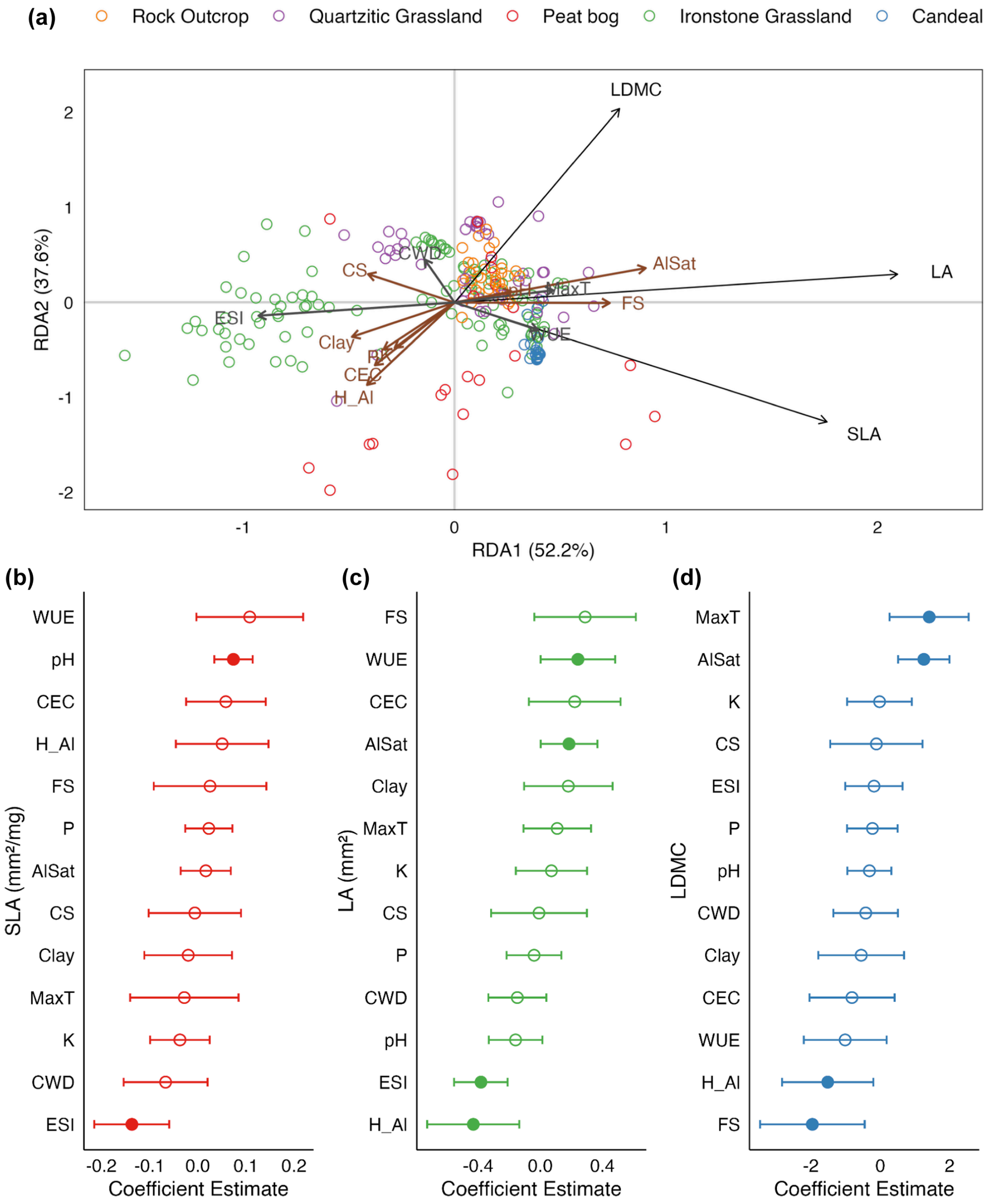

Figure 2. Environmental predictors of variation in leaf traits in the Campo Rupestre, an OCBIL (Old, Climatically buffered, Infertile landscapes) system. (a) Redundancy analysis (RDA) showing how soil and climatic gradients structure community-level variation in specific leaf area (SLA), leaf area (LA) and leaf dry matter content (LDMC). Vectors represent environmental predictors and their loadings on the first two constrained axes. Standardised coefficients from generalised least squares models for (b) $\log_{10}$-transformed SLA, (c) $\log_{10}$-transformed LA and (d) LDMC. Points are model estimates (Supporting information) and horizontal bars denote 95 % confidence intervals; filled points indicate $p < 0.05$. Environmental variables include aluminum saturation (AlSat), coarse sand (CS), fine sand (FS), exchangeable acidity (H_Al), potential of hydrogen (pH), effective cation exchange capacity (CEC), phosphorus (P), potassium (K), maximum temperature (MaxT), water use efficiency (WUE), climate water deficit (CWD), evaporative stress index (ESI).

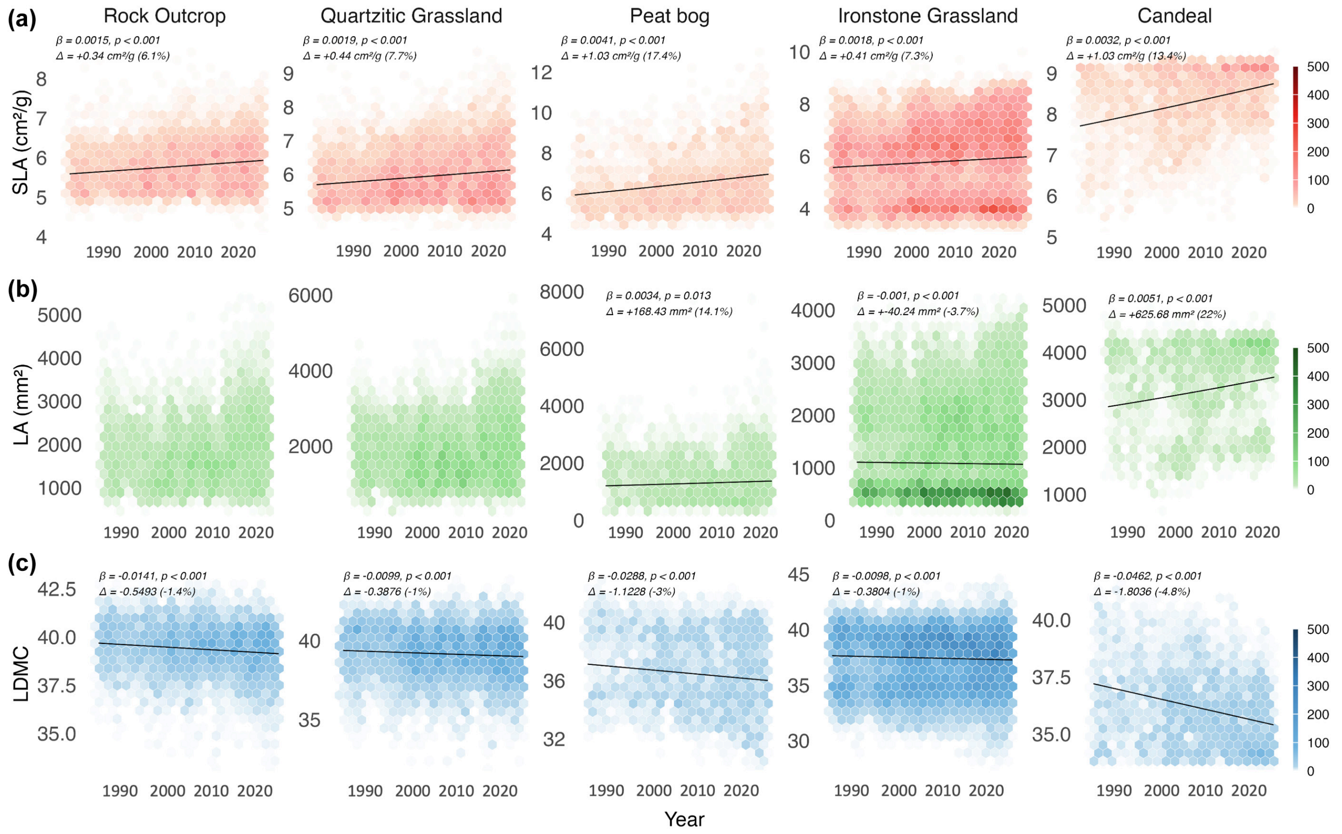

Figure 3. Hindcast of three key leaf functional traits across distinct habitats in the Campo Rupestre, an OCBIL (Old, Climatically buffered, Infertile landscapes), from 1984 to 2022, based on spectral reflectance. Each row corresponds to a trait, (a) specific leaf area (SLA, $cm^2\ g^{-1}$), (b) leaf area (LA, mm^2), and (c) leaf dry matter content (LDMC, %), and each column represents a habitat: Candeal, Ironstone Grasslands, Rock Outcrop, Peat bog and Quartzitic Grasslands. Trait values were hindcast using linear mixed-effects models fitted separately for each trait, with a random intercept for each plot. Hexagons represent annual hindcast values per plot, and black lines show model-predicted temporal trends. Values above each panel give the habitat specific slope of year (β), its p-value, and the absolute and proportional change (Δ) over time.

< 0.001, $R^2m = 0.23$, $R^2c = 0.76$, Fig. 3a). SLA increased in all habitats, with cumulative changes of 6.1% in Rock Outcrop ($\beta = 0.0015\ year^{-1}$, $p < 0.001$), 7.7% in Quartzitic Grassland ($\beta = 0.0019\ year^{-1}$, $p < 0.001$), 17.4% in Peat bog ($\beta = 0.0041\ year^{-1}$, $p < 0.001$) and 7.3% in Ironstone Grassland ($\beta = 0.0018$, $p < 0.001$). Candeal, the model reference habitat, showed a 13.4% increase, corresponding to the baseline temporal trend ($\beta = 0.0032\ year^{-1}$, $p < 0.001$).

Predicted LA values, exhibited habitat-dependent temporal trajectories, reflecting divergent temporal trends among habitats ($\chi^2 = 455.1$, $p < 0.001$, $R^2m = 0.25$, $R^2c = 0.72$, Fig. 3b). In Rock Outcrop and Quartzitic Grassland, predicted LA increased by 21.0 and 21.9%, respectively ($\beta = 0.0049$ and $0.0051\ year^{-1}$, both $p < 0.001$). Peat bog showed a significant increase of 14.1% ($\beta = 0.0034\ year^{-1}$, $p < 0.001$), whereas Ironstone Grassland exhibited a significant decline of 3.7% in predicted LA ($\beta = -0.0010\ year^{-1}$, $p < 0.001$). The reference habitat, Candeal, experienced the strongest increase in LA, with a cumulative rise of 22.0% over the study period ($\beta = 0.0051\ year^{-1}$, $p < 0.001$).

Predicted LDMC values exhibited small but consistent temporal declines across all habitats, with habitat-dependent rates of change ($\chi^2 = 456.1$, $p < 0.001$; $R^2m = 0.21$, $R^2c = 0.69$, Fig. 3c). Over the study period, LDMC decreased by 1.4% in Rock Outcrop ($\beta = -0.0141\ year^{-1}$, $p < 0.001$) and by 1.0% in Quartzitic Grassland ($\beta = -0.0098\ year^{-1}$, $p < 0.001$). Peat bog showed a stronger decline of 3.0% ($\beta = -0.0288\ year^{-1}$, $p < 0.001$), while Ironstone Grassland exhibited a 1.0% decrease ($\beta = -0.0097\ year^{-1}$, $p < 0.001$). Candeal, the reference habitat, displayed the steepest decline in predicted LDMC, with a 4.9% reduction over the study period ($\beta = -0.0462\ year^{-1}$, $p < 0.001$).

Discussion

Functional divergence within a conservatively structured flora in the Campo Rupestre

As expected for OCBIL systems and consistent with previous work in the Campo Rupestre and other nutrient-impoverished tropical ecosystems, community foliar traits indicate a predominantly conservative leaf economics strategy (Hopper 2009, Negreiros et al. 2014, Silveira et al. 2016). Nevertheless, habitats differ in their position within CSR space: although most communities cluster along the C–S edge and are strongly skewed towards the S corner – consistent with pervasive edaphic and climatic stress across the landscape – they still exhibit subtle but meaningful differentiation in the balance among C, S, and (occasionally) R components. By jointly analysing multiple habitats within a single OCBIL ecosystem (Hopper 2009), we show that strong environmental filtering does not entail functional uniformity; rather, it structures habitat-level functional differentiation across fine spatial scales, supporting H1.

Rock Outcrop, Ironstone Grassland and Quartzitic Grassland form a cohesive functional group located at the extreme conservative end of the C–S axis in CSR space and characterised by small leaves, high tissue density, and low SLA. These traits enhance leaf persistence and limit resource loss, placing these communities at the conservative end of the global leaf economics spectrum (Wright et al. 2004, Poorter et al. 2009). Candeal largely shares this conservative profile but displays proportionally larger leaves and slightly lower LDMC, reflecting a displacement along the C–S axis towards higher turnover strategies and more dynamic resource uptake (Grime and Pierce 2012, Qi et al. 2018). In contrast, Peat bog exhibits the broadest functional range among the habitats, encompassing both species with conservative leaf traits and others with larger, less dense leaves indicative of more acquisitive strategies. This functional heterogeneity likely reflects seasonal hydrological fluctuations that may locally relax abiotic filtering, allowing the establishment of opportunistic species and favouring ruderal traits. This interpretation aligns with Grime's prediction that temporal fluctuations in resource availability can promote R-selected strategies within otherwise stress-prone systems (Westoby et al. 2002, Pierce et al. 2017). Altogether, this functional mosaic reveals that landscape-scale conservatism can coexist with habitat-level trait variation, providing a mechanistic basis for understanding biodiversity persistence under chronic environmental stress in the Campo Rupestre.

Edaphic and climatic gradients structure spatial variation in foliar traits

Spatial variation in community-weighted foliar traits across the Campo Rupestre was structured by combined edaphic and climatic gradients, supporting H2. Across the landscape, soil properties defined the primary conservative–acquisitive axis, while climatic water balance modulated trait expression along a secondary gradient. This pattern suggests that climatic variability amplifies or constrains trait expression within edaphically defined limits rather than redefining the functional space available to communities. This hierarchy aligns with evidence that soil texture, acidity, and nutrient limitation act as persistent filters in the Campo Rupestre across fine spatial scales (Silveira et al. 2016), and is consistent with the expectation that warmer and drier conditions reinforce conservative trait combinations already favoured by substrate constraints. Trait-specific models further indicate that SLA, LA and LDMC respond to partially overlapping – but not identical – environmental predictors, implying asymmetric sensitivities to soil chemistry and climatic stress and a degree of partial decoupling among leaf traits, as reported in broader syntheses of trait coordination under resource limitation (Wright et al. 2004, Díaz et al. 2016, Messier et al. 2017). Accordingly, habitats occupied distinct yet continuous regions of constrained trait-environment space, indicating differentiation along gradients rather than discrete habitat-specific syndromes. The remaining unexplained variation likely reflects additional fine-scale heterogeneity, species turnover and intraspecific trait variation (Negreiros et al. 2014, Siefert et al. 2015, Silveira et al. 2016). Overall, functional diversity in the Campo Rupestre emerges from – rather than despite – strong environmental constraints, because persistent soil gradients and water-balance variation structure continuous trait differentiation across the landscape (Díaz et al. 2007).

Retrospective projections reveal constrained temporal reorganisation of foliar traits in Campo Rupestre communities

H3 predicted that present-day communities would exhibit more conservative trait profiles than in the past, reflecting increasing environmental stress through time. By hindcasting historical trait values from long-term satellite reflectance, we reconstructed four decades of community-level trait trajectories and evaluated temporal shifts in foliar trait composition. Contrary to this expectation, we observed a weakening of conservative trait expression, characterised by consistent increases in SLA and LA and concomitant reductions in LDMC across several habitats, despite clear evidence of increasing climatic stress over the study period in the Campo Rupestre.

This temporal reorganisation is consistent with two non-exclusive mechanisms: phenotypic plasticity and slow shifts in species composition. Phenotypic plasticity may enable fine-scale adjustments in trait expression within species in response to environmental change (Messier et al. 2017, Weng et al. 2021), whereas shifts in floristic composition likely reflect gradual selective processes favouring the establishment and persistence of species with trait syndromes pre-adapted to these conditions (Bertrand et al. 2011, Gottfried et al. 2012, Feeley et al. 2020). However, in an OCBIL system dominated by long-lived species and strong edaphic filtering, such compositional change is expected to occur slowly and within a narrow functional space. Under these constraints, the observed shift away from conservative trait combinations likely reflects a gradual reduction in the relative dominance of the most conservative species, rather than the establishment of highly acquisitive species. Among these selective forces acting against conservative species, fire represents a particularly relevant but unmodelled factor in the Campo Rupestre. Fire is a recurrent and spatially variable disturbance in this system and has been shown to favour acquisitive trait combinations associated with faster post-disturbance recovery, including higher SLA, lower LDMC and shorter leaf lifespan, especially in Quartzitic and Ironstone Grasslands (Moura et al. 2023).

Finally, these inferences are based on predictive models derived from remotely sensed reflectance and therefore carry uncertainty, particularly in heterogeneous landscapes with complex species mixtures. Spectral signals integrate not only trait variation but also phenology, canopy structure, and background effects, which can obscure fine-scale functional dynamics. While our results suggest strong constraints on temporal functional reorganisation in Campo Rupestre communities, they also underscore the value of long-term field monitoring and multi-scale approaches to validate and refine trait-based projections in OCBIL ecosystems.

In summary, our results show that Campo Rupestre communities are functionally conservative at the landscape scale, yet finely structured by persistent edaphic and microclimatic gradients and capable of modest, context-dependent reorganisation through time. Strong environmental filters maintain communities within a predominantly stress-tolerant region of trait space while still allowing habitat-level functional differentiation. Although climatic indicators point to increasing warming and drought stress over the study period -leading to the expectation of progressively more conservative community trait profiles – our retrospective projections instead reveal only subtle temporal shifts, and in several habitats a modest weakening of conservative expression (higher SLA and LA, lower LDMC). Temporal variation remains small relative to spatial differentiation, suggesting substantial functional inertia through time. These patterns are most consistent with constrained flexibility arising from within-species plasticity and slow compositional change, potentially modulated by disturbance (e.g. spatially variable fire regimes). Overall, this combination of functional inertia and limited reorganisation implies that biodiversity persistence in the Campo Rupestre may depend less on wholesale strategy shifts and more on the reconfiguration of conservative trait syndromes within a narrow, environmentally defined functional domain.

Acknowledgements – We are also grateful to the researchers of the Laboratory of Evolutionary Ecology and Biodiversity (LEEB–UFMG), especially Jéssica Cunha-Blum, Dario Paiva and Vanessa Gomes, for their substantial contributions to data collection and database construction, and to Reserva Vellozia for logistical support.
Funding – This work was supported by Anglo American; by Conselho Nacional de Desenvolvimento Científico e Tecnológico (CNPq), Brazil, through PPBio-ComCerrado (grant no. 442499/2023-0), PELD-CRSC (grant no. 441569/2024-7), PELD-CRAM (grant no. 446002/2024-0), and the Knowledge Center for Biodiversity (INCT/CNPq grant no. 406757/2022-4); and by Fundação de Amparo à Pesquisa em Minas Gerais (FAPEMIG), Brazil, through PELD-CRSC (grant no. 2070.01./04464/2025-35). R.M. and M.B were also supported by CNPq (grant no.403055/2022-9).
Conflict of interest – The authors declare no conflict of interest.

Author contributions

Renata Maia: Conceptualization (lead); Data curation (lead); Formal analysis (lead); Investigation (lead); Methodology (lead); Software (lead); Validation (lead); Visualization (lead); Writing – original draft (lead). **Milton Barbosa**: Conceptualization (equal); Data curation (equal); Formal analysis (equal); Investigation (equal); Methodology (equal); Software (equal); Validation (equal); Visualization (equal); Writing – review and editing (equal). **Daniel Negreiros**: Conceptualization (equal); Data curation (equal); Formal analysis (equa); Investigation (equal); Methodology (equal); Resources (equal); Software (equal); Validation (equal); Visualization (equal); Writing – review and editing (equal). **Geraldo Wilson Fernandes**: Data curation (equal); Funding acquisition (lead); Investigation (equal); Methodology (equal); Project administration (equal); Resources (lead); Validation (equal); Writing – review and editing (equal). **Yadvinder Malhi**: Investigation (equal); Writing – review and editing (equal). **Jesús Aguirre-Gutiérrez**: Conceptualization (equal); Formal analysis (equal); Investigation (equal); Methodology (equal); Software (equal); Supervision (equal); Validation (equal); Visualization (equal); Writing – review and editing (equal).

Transparent peer review

The peer review history for this article is available at https://www.webofscience.com/api/gateway/wos/peer-review/ecog.07634.

Data availability statement

Data are available from Zenodo: https://doi.org/10.5281/zenodo.18165398 (Maia et al. 2026).

Supporting information

The Supporting information associated with this article is available with the online version.

References

Abatzoglou, J. T., Dobrowski, S. Z., Parks, S. A. and Hegewisch, K. C. 2018. TerraClimate, a high-resolution global dataset of monthly climate and climatic water balance from 1958–2015. – Sci. Data 5: 170191.

Aguirre-Gutiérrez, J. et al. 2021. Pantropical modelling of canopy functional traits using Sentinel-2 remote sensing data. – Remote Sens. Environ. 252: 112122.

Aguirre-Gutiérrez, J. et al. 2025. Tropical forests in the Americas are changing too slowly to track climate change. – Science 387: eadl5414.

Alvares, C. A., Stape, J. L., Sentelhas, P. C., De Moraes Gonçalves, J. L. and Sparovek, G. 2013. Köppen's climate classification map for Brazil. – Metz 22: 711–728.

Anderson, M. C., Hain, C., Wardlow, B., Pimstein, A., Mecikalski, J. R. and Kustas, W. P. 2011. Evaluation of drought indices based on thermal remote sensing of evapotranspiration over the continental United States. – National Drought Mitigation Center: Faculty Publications.

Barbosa, N. P. de U., Fernandes, G. W. and Sanchez-Azofeifa, A. 2015. A relict species restricted to a quartzitic mountain in tropical America: an example of microrefugium? – Acta Bot. Bras. 29: 299–309.

Bertrand, R., Lenoir, J., Piedallu, C., Riofrío-Dillon, G., de Ruffray, P., Vidal, C., Pierrat, J.-C. and Gégout, J.-C. 2011. Changes in plant community composition lag behind climate warming in lowland forests. – Nature 479: 517–520.

Caminha-Paiva, D., Negreiros, D., Barbosa, M. and Fernandes, G. W. 2021. Functional trait coordination in the ancient and nutrient-impoverished campo rupestre: soil properties drive stem, leaf and architectural traits. – Biol. J. Linn. Soc. 133: 531–545.

Corlett, R. T. and Tomlinson, K. W. 2020. Climate change and edaphic specialists: irresistible force meets immovable object? – Trends Ecol. Evol. 35: 367–376.

Crawford, C. J., Roy, D. P., Arab, S., Barnes, C., Vermote, E., Hulley, G. and Zahn, S. 2023. The 50-year Landsat collection 2 archive. – Sci. Remote Sens. 8: 100103.

Díaz, S., Lavorel, S., Chapin III, F. S., Tecco, P. A., Gurvich, D. E. and Grigulis, K. 2007. Functional biodiversity – at the crossroads between responses to the environment and ecosystem functioning. – In: Canadell, J., Pitelka, L. F. and Pataki, D. (eds), Terrestrial ecosystems in a changing world. Springer.

Díaz, S. et al. 2016. The global spectrum of plant form and function. – Nature 529: 167–171.

Donagemma, G., K., Viana, J. H. M., Almeida, B. G. and Ruiz, H. A. 2017. Análise granulométrica. – In: Teixeira, P. C. et al. (eds), Manual de métodos de análise de solo, 3rd edn. Embrapa Solos, pp. 95–116.

Feeley, K. J., Bravo-Avila, C., Fadrique, B., Perez, T. M. and Zuleta, D. 2020. Climate-driven changes in the composition of New World plant communities. – Nat. Clim. Change 10: 965–970.

Fernandes, G. W. 2016. The megadiverse rupestrian grassland. – In: Fernandes, G. W. (ed.), Ecology and conservation of mountaintop grasslands in Brazil. Springer.

Fernandes, G. W. et al. 2020. Biodiversity and ecosystem services in the Campo Rupestre: a road map for the sustainability of the hottest Brazilian Biodiversity Hotspot. – Perspect. Ecol. Conserv. 18: 213–222.

Fisher, J. B. et al. 2020. ECOSTRESS: NASA's next generation mission to measure evapotranspiration from the international space station. – Water Resour. Res. 56: WR026058: e2019.

Gottfried, M. et al. 2012. Continent-wide response of mountain vegetation to climate change. – Nat. Clim. Change 2: 111–115.

Grime, J. P. 1977. Evidence for the existence of three primary strategies in plants and its relevance to ecological and evolutionary theory. – Am. Nat. 111: 1169–1194.

Grime, J. P. and Pierce, S. 2012. The evolutionary strategies that shape ecosystems. – John Wiley and Sons.

Hopper, S. D. 2009. OCBIL theory: towards an integrated understanding of the evolution, ecology and conservation of biodiversity on old, climatically buffered, infertile landscapes. – Plant Soil 322: 49–86.

Hopper, S. D. 2021. Out of the OCBILs: new hypotheses for the evolution, ecology and conservation of the eucalypts. – Biol. J. Linn. Soc. 133: 342–372.

Huntley, B., Barnard, P., Altwegg, R., Chambers, L., Coetzee, B. W. T., Gibson, L., Hockey, P. A. R., Hole, D. G., Midgley, G. F., Underhill, L. G. and Willis, S. G. 2010. Beyond bioclimatic envelopes: dynamic species' range and abundance modelling in the context of climatic change. – Ecography 33: 621–626.

Jacobi, C. M., do Carmo, F. F., Vincent, R. C. and Stehmann, J. R. 2007. Plant communities on ironstone outcrops: a diverse and endangered Brazilian ecosystem. – Biodivers. Conserv. 16: 2185–2200.

Kattenborn, T., Fassnacht, F. E., Pierce, S., Lopatin, J., Grime, J. P. and Schmidtlein, S. 2017. Linking plant strategies and plant traits derived by radiative transfer modelling. – J. Veg. Sci. 28: 717–727.

Kattenborn, T., Fassnacht, F. E. and Schmidtlein, S. 2019. Differentiating plant functional types using reflectance: which traits make the difference? – Remote Sens. Ecol. Conserv. 5: 5–19.

Kuhn, M. 2008. Building predictive models in R using the caret package. – J. Stat. Softw. 28: 1–26.

Laliberté, E., Legendre, P. and Shipley, B. 2014. FD: measuring functional diversity (FD) from multiple traits, and other tools for functional ecology. – R package, ver. 1.0-12.3, https://CRAN.R-project.org/package=FD.

Lambers, H., Chapin, F. S. and Pons, T. L. 2008. Plant physiological ecology. – Springer.

Lenth, R. V. 2025. emmeans: estimated marginal means, aka least-squares means. – R package, DOI: 10.32614/CRAN.package.emmeans.

Liaw, A. and Wiener, M. 2002. Classification and regression by randomForest. – R News 2: 18–22.

Ma, Z., Liu, H., Mi, Z., Zhang, Z., Wang, Y., Xu, W., Jiang, L. and He, J.-S. 2017. Climate warming reduces the temporal stability of plant community biomass production. – Nat. Commun. 8: 15378.

Madeira, J. A. and Fernandes, G. W. 1999. Reproductive phenology of sympatric taxa of *Chamaecrista* (Leguminosae) in Serra do Cipó, Brazil. – J. Trop. Ecol. 15: 463–479.

Maia, R., Barbosa, M., Negreiros, D., Fernandes, G., Malhi, Y. and Aguirre Gutiérrez, J. 2026. Satellite hindcasts of foliar traits reveal a subtle but consistent relaxation of conservativeness in a biodiverse mountain grassland over the last four decades [Data set]. – Zenodo, https://doi.org/10.5281/zenodo.18165398.

Messier, J., Lechowicz, M. J., McGill, B. J., Violle, C. and Enquist, B. J. 2017. Interspecific integration of trait dimensions at local scales: the plant phenotype as an integrated network. – J. Ecol. 105: 1775–1790.

Moura, A. L., Negreiros, D. and Fernandes, G. W. 2023. Effects of fire frequency regimes on flammability and leaf economics of non-graminoid vegetation. – Fire 6: 265.

Nakagawa, S. and Schielzeth, H. 2013. A general and simple method for obtaining R^2 from generalized linear mixed-effects models. – Methods Ecol. Evol. 4: 133–142.

Negreiros, D., Le Stradic, S., Fernandes, G. W. and Rennó, H. C. 2014. CSR analysis of plant functional types in highly diverse tropical grasslands of harsh environments. – Plant Ecol. 215: 379–388.

Ordway, E. M., Asner, G. P., Burslem, D. F. R. P., Lewis, S. L., Nilus, R., Martin, R. E., O'Brien, M. J., Phillips, O. L., Qie, L., Vaughn, N. R. and Moorcroft, P. R. 2022. Mapping tropical forest functional variation at satellite remote sensing resolutions depends on key traits. – Commun. Earth Environ. 3: 1–11.

Paiva, D. C., Negreiros, D., Cunha-Blum, J., Rago, C., Gomes, V. M., Gélvez-Zúñiga, I. and Fernandes, G. W. 2025. Unraveling the influence of soil properties on CSR strategies in an ironstone montane ecosystem in southeast Brazil. – J. Veg. Sci. 36: e70092.

Pérez-Harguindeguy, N. et al. 2013. New handbook for standardised measurement of plant functional traits worldwide. – Aust. J. Bot. 61: 167–234.

Pierce, S. et al. 2017. A global method for calculating plant CSR ecological strategies applied across biomes world-wide. – Funct. Ecol. 31: 444–457.

Pinheiro, J., Bates, D. and R Core Team 2025. nlme: linear and nonlinear mixed effects models. – R package, DOI: 10.32614/CRAN.package.nlme.

Poorter, H., Niinemets, Ü., Poorter, L., Wright, I. J. and Villar, R. 2009. Causes and consequences of variation in leaf mass per area (LMA): a meta-analysis. – New Phytol. 182: 565–588.

Povak, N. A. and Manley, P. N. 2024. Evaluating climate change impacts on ecosystem resources through the lens of climate analogs. – Front. For. Global Change 6: 1–19.

Qi, M., Sun, T., Xue, S., Yang, W., Shao, D. and Martínez-López, J. 2018. Competitive ability, stress tolerance and plant interactions along stress gradients. – Ecology 99: 848–857.

Querejeta, J. I., Ren, W. and Prieto, I. 2021. Vertical decoupling of soil nutrients and water under climate warming reduces plant cumulative nutrient uptake, water-use efficiency and productivity. – New Phytol. 230: 1378–1393.

Rapini, A., Bitencourt, C., Luebert, F. and Cardoso, D. 2021. An escape-to-radiate model for explaining the high plant diversity and endemism in campos rupestres. – Biol. J. Linn. Soc. 133: 481–498.

Rios, C. O., Pimentel, P. A., Živčák, M., Brestič, M. and Pereira, E. G. 2022. Can ecological strategies be explained by photochemical efficiency in ironstone outcrops vegetation? – Plant Soil 480: 105–120.

Rummukainen, M. 2012. Changes in climate and weather extremes in the 21st century. – Wiley Interdiscip. Rev. Clim. Change 3: 115–129.

Schielzeth, H. 2010. Simple means to improve the interpretability of regression coefficients. – Methods Ecol. Evol. 1: 103–113.

Siefert, A. et al. 2015. A global meta-analysis of the relative extent of intraspecific trait variation in plant communities. – Ecol. Lett. 18: 1406–1419.

Silva, F. C. da, Eira, P. A. da, Barreto, W. de O., Perez, D. V. and Silva, C. A. 1999. Análises químicas para avaliação da fertilidade do solo. – In: Silva, F. C. (ed.), Manual de análises químicas de solos, plantas e fertilizantes. Embrapa, pp. 75–169.

Silveira, F. A. O. et al. 2016. Ecology and evolution of plant diversity in the endangered campo rupestre: a neglected conservation priority. – Plant Soil 403: 129–152.

Silveira, F. A. O., Dayrell, R. L. C., Fiorini, C. F., Negreiros, D. and Borba, E. L. 2020. Diversification in ancient and nutrient-poor Neotropical ecosystems: how geological and climatic buffering shaped plant diversity in some of the world's neglected hotspots. – In: Rull, V. and Carnaval, A. C. (eds), Neotropical diversification: patterns and processes. Fascinating life sciences. Springer, pp. 329–368.

Tameirão, L. B. S., Caminha-Paiva, D., Negreiros, D., Veloso, M. D. D. M., Berbara, R. L. L., Dias, L. E., Pierce, S. and Fernandes, G. W. 2021. Role of environmental filtering and functional traits for species coexistence in a harsh tropical montane ecosystem. – Biol. J. Linn. Soc. 133: 546–560.

Trenberth, K. E., Dai, A., van der Schrier, G., Jones, P. D., Barichivich, J., Briffa, K. R. and Sheffield, J. 2014. Global warming and changes in drought. – Nat. Clim. Change 4: 17–22.

Walkley, A. and Black, I. A. 1934. An examination of the Degtjareff method for determining soil organic matter, and a proposed modification of the chromic acid titration method. – Soil Sci. 37: 29–38.

Wang, Z., Chlus, A., Geygan, R., Ye, Z., Zheng, T., Singh, A., Couture, J. J., Cavender-Bares, J., Kruger, E. L. and Townsend, P. A. 2020. Foliar functional traits from imaging spectroscopy across biomes in eastern North America. – New Phytol. 228: 494–511.

Weng, J. K., Lynch, J. H., Matos, J. O. and Dudareva, N. 2021. Adaptive mechanisms of plant specialized metabolism connecting chemistry to function. – Nat. Chem. Biol. 17: 1037–1045.

Westoby, M., Falster, D. S., Moles, A. T., Vesk, P. A. and Wright, I. J. 2002. Plant ecological strategies: some leading dimensions of variation between species. – Annu. Rev. Ecol. Syst. 33: 125–159.

Wright, I. J. et al. 2004. The worldwide leaf economics spectrum. – Nature 428: 821–827.